$$W_K(\Theta) = \Theta_K{}^{M_K} F_{0K}(\mathbf{u}) \quad (52)$$

$$\mathbf{u} = (\mathbf{u}_A, ..., \mathbf{u}_K...)$$

$$\mathbf{u}_K = (u_{K,v}, u_{K,1-v})$$

$$u_{K,v} = \Theta_{K,v}{}^{M_K} F_{K,v}(\mathbf{u})$$

$$u_{K,1-v} = \Theta_{K,1-v}{}^{M_K} F_{K,1-v}(\mathbf{u})$$

$$\Theta_K = v_K \Theta_{K,v} + (1 - v_K)\Theta_{K,1-v}$$

where M_K is the molecular weight of the unit of type K, F_K is the pgf for the number of bonds issuing from a unit of type K on generation g to a unit on generation $g + 1$, provided $g > 0$. The weight-average molecular weight is then obtained by the differentiation of eq 52 with respect to all variables given by the vector Θ for $\Theta = 1$.

Another case of interest is the vulcanization of chains with an arbitrary degree of polymerization distribution. It is possible to take the whole primary chains as roots, a method suggested originally by Dobson and Gordon,[12] and to find the number of active branch points, units of EANC's, and of dangling chains assuming a random distribution of cross-linked units along the primary chain, which determines the degree of polymerization distribution of parts of primary chains between cross-links.

The other possibility for determining the DP averages of EANC's and dangling chains can be found by taking every monomer unit of primary chains as a root and constructing the weight-fraction gf in the same way as that employed in treating cross-linking and degradation.[25] The latter method is more straightforward for calculating the higher moments of the DP distribution.

References and Notes

(1) Flory, P. J. *Proc. R. Soc. London, Ser. A* **1976**, *351*, 351.
(2) Flory, P. J. *Polymer* **1979**, *20*, 1317.
(3) Flory, P. J. *Macromolecules* **1982**, *15*, 99.
(4) Dušek, *Makromol. Chem.* **1979**, *Suppl. 2*, 35.
(5) Dušek, K. *Rubber Chem. Technol.* **1982**, *55*, 1.
(6) Ferry, J. D. "Viscoelastic Properties of Polymers"; Wiley: New York, 1970.
(7) Mooney, M. *J. Polym. Sci.* **1959**, *34*, 599.
(8) Cohen, R. E.; Tschoegl, N. W. *Int. J. Polym. Mater.* **1972**, *2*, 49; **1973**, *3*, 205.
(9) Bibbó, M. A.; Vallés, E. M. *Macromolecules* **1982**, *15*, 1300.
(10) Havránek, A.; Nedbal, J.; Berčík, Č.; Ilavský, M.; Dušek, K. *Polym. Bull.* **1980**, *3*, 497; unpublished results.
(11) Flory, P. J. "Principles of Polymer Chemistry"; Cornell University Press: Ithaca, NY, 1950.
(12) Dobson, G. R.; Gordon, M. *J. Chem. Phys.* **1965**, *43*, 705.
(13) Gordon, M. *Proc. R. Soc. London, Ser. A* **1962**, *268*, 240.
(14) Gordon, M.; Malcolm, G. N. *Proc. R. Soc. London* **1966**, *295*, 29.
(15) Dušek, K.; Prins, W. *Adv. Polym. Sci.* **1969**, *6*, 1.
(16) Burchard, W. *Adv. Polym. Sci.* **1983**, *48*, 1.
(17) Macosko, C. W.; Miller, D. R. *Macromolecules* **1976**, *9*, 199.
(18) Miller, D. R.; Macosko, C. W. *Macromolecules* **1976**, *9*, 206.
(19) Stockmayer, W. H. *J. Chem. Phys.* **1943**, *11*, 45.
(20) Stockmayer, W. H. *J. Chem. Phys.* **1944**, *12*, 125.
(21) Kuchanov, S. I. "Methods of Kinetic Calculations in Polymer Chemistry"; Khimiya: Moscow, 1978 (in Russian).
(22) Dušek, K. *Polym. Bull.* **1979**, *1*, 523.
(23) Mikeš, J.; Dušek, K. *Macromolecules* **1982**, *15*, 99.
(24) Dušek, K.; Gordon, M.; Ross-Murphy, S. B. *Macromolecules* **1978**, *11*, 236.
(25) Dušek, K.; Demjanenko, M. *Macromolecules* **1980**, *13*, 571.

Further Studies of Spin Relaxation and Local Motion in Dissolved Polycarbonates

John J. Connolly, Edward Gordon, and Alan Anthony Jones*

Jeppson Laboratory, Department of Chemistry, Clark University, Worcester, Massachusetts 01610.

Received June 14, 1983

ABSTRACT: Both proton and carbon-13 spin–lattice relaxation times at two fields are reported for dilute solutions of two polycarbonates. For the polycarbonate of 2,2-propanediylbis(4-hydroxyphenyl) carbonate, the relaxation measurements were made as a function of concentration in $C_2D_2Cl_4$ and temperature while for the polycarbonate of 1,1-dichloro-2,2-bis(4-hydroxyphenyl)ethylene the measurements were made at a concentration of 10 wt % in $C_2D_2Cl_4$ and as a function of temperature. A partially deuterated analogue of the first polycarbonate was made to remove cross-relaxation effects from the proton relaxation. The proton and carbon-13 relaxation times are interpreted in terms of three local motions: segmental motion, phenyl group rotation, and methyl group rotation. Two different correlation functions are employed for segmental motion. An older function based on the three-bond jump and a new function by Weber and Helfand gave successful interpretations, yielding surprising similar conclusions concerning segmental motion. Both segmental interpretations relied primarily on cooperative backbone transitions, yielding similar time scales and apparent activation energies for this type of motion. Estimates of the time scale for phenyl group rotation and methyl group rotation did not depend on the model used for segmental motion. By and large the time scale for phenyl group rotation paralleled the time scale for segmental motion as temperature and concentration changed while methyl group rotation displayed a weaker concentration dependence.

Introduction

Two reports of spin relaxation and local motion of dissolved polycarbonates have already been made[1,2] but a more complete series of observations is presented now to verify and expand the previous interpretations. In addition, a new correlation function for segmental motion developed by Weber and Helfand[3] is tested and compared to an earlier function based on the three bond jump.[4] The large data base given for polycarbonates is well suited for test applications of models though the repeat unit structure of the polycarbonates is more complex than the basis of either model.

Specific improvements in the data set relative to the earlier reports[1,2] include the addition of carbon-13 spin–

0024-9297/84/2217-0722$01.50/0

Table I
Phenyl Proton Spin-Lattice Relaxation Times of BPA-d_6[a]

	90 MHz			22.6 MHz		
temp, °C	5 wt %	10 wt %	30 wt %	5 wt %	10 wt %	30 wt %
−20	613	665		175	160	
0	590	614	699	222	180	168
20	666	626	631	308	238	165
40	817	723	600	409	253	182
60	993	868	626	542	381	228
80	1227	1008	706	714	526	295
100	1500	1219	802	943	749	384
120	1744	1338	920	1138	869	527

[a] All relaxation times in ms.

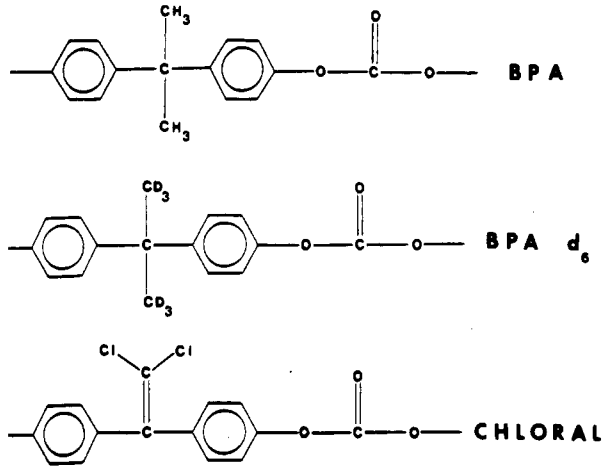

Figure 1. Structures of the repeat units and abbreviations for the three polycarbonates studied.

lattice relaxation times, T_1's, at two field strengths to the proton T_1's at two field strengths, thereby extending the frequency range probed. A partially deuterated form of the polycarbonate of 2,2-propanediylbis(4-hydroxyphenyl) carbonate, shown in Figure 1 and abbreviated BPA, is utilized in the proton measurements to reduce the effects of cross relaxation. The measurements on BPA were also made at concentrations of 5, 10, and 30 wt % in perdeuterio 1,1,2,2-tetrachloroethane. The new solvent $C_2D_2Cl_4$ is used in place of the $CDCl_3$ employed earlier because it allows for measurements over a much greater temperature range. The analogous study of the polycarbonate of 1,1-dichloro-2,2-bis(4-hydroxyphenyl)-ethylene, shown in Figure 1 and abbreviated chloral, is reported here over the same expanded temperature and frequency range.

The interpretation of the spin relaxation times in these polycarbonates follows the same prescription as the earlier reports and yields similar conclusions.[1,2] However, these conclusions should be more credible now as a result of the improved and expanded data base. Probably the most definitive improvement in the data stems from the use of BPA-d_6 (methyl protons replaced with deuterons) and thus the elimination of cross relaxation between the methyl and phenyl protons. The concentration dependence of the BPA data is also of interest since it tests the possibility of coupling of local motions as the time scales of these motions are shifted by intermolecular interactions.

The use of two models for segmental motion also reinforces the earlier interpretation since both models lead to very similar descriptions of the local motions in these polycarbonates. Though at first glance the model parameters seem quite different, they both place the main burden of the interpretation on cooperative backbone transitions and produce similar time scales for these motions. Unfortunately, the spin relaxation data in hand cannot distinguish between these two models on the basis of the quality of the fit or simulation. These difficulties in discriminating between models for segmental motion have been noted before[5,6] but one can check the new model by Weber and Helfand[3] to see if it leads to a reasonable characterization of segmental motion as temperature and concentration are changed.

Experimental Section

High molecular weight samples of the two polycarbonates were kindly supplied by General Electric. The structures of the repeat units are given in Figure 1 as well as the structure of the partially deuterated form of BPA. Samples were prepared as 5, 10, and 30 wt % solutions in $C_2D_2Cl_4$ and were subjected to five freeze–pump–thaw cycles before sealing.

Two spectrometers were used. The proton measurements and the 22.6-MHz carbon-13 measurements were made on a variable-field Bruker SXP 20-100. The 62.9-MHz carbon-13 measurements were made on a Bruker WM-250. All T_1 measurements were made with a standard 180°–τ–90° sequence and are reported with an experimental uncertainty of 10%. This includes errors arising from sample preparation and temperature control as well as from the pulse sequence and the fitting of the return of the magnetization to equilibrium.

Results

The return of the magnetization to equilibrium monitored in the 180°–τ–90° sequence was assumed to follow a simple exponential dependence on delay time, τ. The data were fit both with the standard linear least-squares form and with a more general nonlinear three-parameter fit. By and large, the same values for T_1 were found from both fits, and average values are reported. A slightly more complicated behavior is observed for the methyl protons and carbons in solutions of BPA. Here a slight upward curvature is noticed if the data are plotted in the form ln $(A_\infty - A_\tau)$ vs. τ. This curvature most likely results from cross correlation among the methyl protons associated with "rapid" methyl group rotation. Methyl group rotation is least affected by increasing concentration and becomes faster than other local motions at higher concentrations; indeed the upward curvature is most noticeable in the 30 wt % case. Cross-correlation complications can be removed by considering only the initial part of the decay curve ($\tau < T_1$) and the values of methyl data reported here are so corrected.[7]

As in the earlier studies, both protonated phenyl carbons have the same T_1 within experimental error, so only one value is reported. Spin–lattice relaxation times for BPA are presented in Tables I–IV and those for chloral are presented in Table V.

Interpretation

The standard relationships between T_1's and spectral densities, J, are employed. For carbon-13, the expressions are[2]

$$1/T_1 = W_0 + 2W_{1C} + W_2$$

$$W_0 = \sum_j \gamma_C^2\gamma_H^2\hbar^2 J_1(\omega_0)/20r_j^6$$

$$W_{1C} = \sum_j 3\gamma_C^2\gamma_H^2\hbar^2 J_1(\omega_C)/40r_j^6 \qquad (1a)$$

$$W_2 = \sum_j 3\gamma_C^2\gamma_H^2\hbar^2 J_2(\omega_2)/10r_j^6$$

$$\omega_0 = \omega_H - \omega_C \qquad \omega_2 = \omega_H + \omega_C$$

and for protons the relationship is

$$1/T_1 = \sum_j (9/8)\gamma^4\hbar r_j^6[(2/15)J_1(\omega_H) + (8/15)J_2(2\omega_H)] \qquad (1b)$$

The internuclear distances employed are 1.09 Å for the phenyl C–H distance, 1.09 Å for the methyl C–H distance, 2.41 Å for the 2–3 phenyl proton distance,[1] and 1.77 Å for the methyl proton–proton distance.

The expressions for the spectral density here are derived from the action of three local motions on intramolecular internuclear interactions. The motions are segmental rearrangements, phenyl group rotation, and methyl group rotation. The geometry of the various internuclear interactions relative to the three motions allows for a separate characterization of each of the motions as described before.[1]

The first description of segmental motion employed in the analysis of the data is derived from the action of a three-bond jump on a tetrahedral lattice with a sharp cutoff of coupling.[4] The time scale of segmental motion is set by adjusting τ_h, the harmonic-average correlation time. The effective distribution of exponential correlation times is controlled by the choice of m, the number of coupled bonds.

Phenyl group rotation is treated as stochastic diffusion about the C_1C_4 axis, with a correlation time τ_{irp} setting the time scale. Methyl group rotation is treated as jumps among three equivalent minima at ϕ and $\phi \pm 120°$, with the correlation time τ_{irm} setting the time scale. If each of the three motions is considered to be independent, the composite spectral density is written as[2]

$$J_1(\omega_i) = 2\sum_{k=1}^{s} G_k \frac{A\tau_{k0}}{1 + \omega_i^2\tau_{k0}^2} + \frac{B\tau_{bk0}}{1 + \omega_i^2\tau_{bk0}^2} + \frac{C\tau_{ck0}}{1 + \omega_i^2\tau_{ck0}^2}$$

$$\tau_{k0}^{-1} = \tau_k^{-1}$$

$$\tau_k = W\lambda_k \qquad s = (m + 1)/2$$

$$\lambda_k = 4\sin^2[(2k - 1)\pi/2(m + 1)]$$

$$\tau_h^{-1} = 2W$$

$$G_k = 1/s + (2/s)\sum_{q=1}^{s-1} \exp(-\gamma q)\cos[(2k - 1)\pi q/2s] \qquad (2)$$

$$\gamma = \ln 9$$

$$A = (3\cos^2\Delta - 1)^2/4$$

$$B = 3(\sin^2 2\Delta)/4$$

$$C = 3(\sin^4\Delta)/4$$

For stochastic diffusion

$$\tau_{bk0}^{-1} = \tau_k^{-1} + \tau_{ir}^{-1}$$

$$\tau_{ck0} = \tau_k^{-1} + (\tau_{ir}/4)^{-1}$$

For a threefold jump

$$\tau_{bk0}^{-1} = \tau_{ck0}^{-1} = \tau_k^{-1} + \tau_{ir}^{-1}$$

The angle Δ is between the internuclear vector and the axis of internal rotation.

The method used to simulate the relaxation data and thus determining τ_h, m, τ_{irp}, and τ_{irm} has been presented before. The phenyl proton data at two field strengths are used to set τ_h and m since the phenyl protons relax only by the action of segmental motion.[1] The use of partially deuterated BPA removes cross relaxation between the phenyl protons and methyl protons, improving the assumption of relaxation through segmental motion. Cross relaxation significantly affected the values of the phenyl proton T_1's near the T_1 minimum, so values reported here are more accurate than the earlier reports.[1,2]

After segmental description is set from the phenyl proton data, the correlation time for phenyl group rotation is determined by simulating the phenyl carbon T_1's. These T_1's depend on both segmental motion and phenyl group rotation, but the description of the former has already been fixed by the phenyl proton data. An improvement is also realized relative to the previous studies[1,2] here since there are two phenyl carbon T_1's at 22.63 and 62.9 MHz to match by adjusting τ_{irp}.

Methyl group rotation is the best determined of the simulation parameters since methyl proton and carbon data at two field strengths must be matched by adjusting τ_{irm}. Again the description of segmental motion already developed from the phenyl proton data is assumed, with τ_{irm} being adjusted to match the observed methyl relaxation data. Of course, the chloral polycarbonate contains no methyl group so this last simulation pertains only to BPA but otherwise the same procedure is followed for both polymers.

Few problems were encountered in the simulation, and essentially all the observed values could be reproduced by simulation to within the experimental uncertainty of 10%. Tables VI and VII contain the simulation parameters for BPA and chloral, respectively. One can calculate apparent activation energies from the temperature dependence of the correlation times assuming Arrhenius behavior. These are included in Tables VI and VII.

The whole interpretation can be repeated for spectral densities derived from the new correlation function for segmental motion developed by Weber and Helfand[3] based on computer simulations of chain dynamics. The new correlation function is

$$\phi(t) = \exp(-t/\tau_0)\exp(-t/\tau_1)I_0(t/\tau_1) \qquad (3)$$

where τ_0 is the correlation time for single-bond conformational transitions, τ_1 is the correlation time for cooperative conformational transitions involving several bonds, and I_0 is a modified Bessel function of order zero. The correlation function was determined by considering dynamics of polyethylene-type chains, and the approach leads most directly to a conformational correlation function instead of the correlation function for the second spherical harmonics required for dipole–dipole relaxation. Nevertheless, the overall considerations of chain dynamics leading up to this correlation function are certainly a more realistic basis than earlier developments such as the three-bond jump. The correlation function can be Fourier transformed[8] to yield the following spectral density required for calculations of spin relaxation.

$$J(\omega) = 2\{[(\tau_0^{-1})(\tau_0^{-1} + 2\tau_1^{-1}) - \omega^2]^2 + [2(\tau_0^{-1} + \tau_1^{-1})\omega]^2\}^{-1/4} \times \cos[\tfrac{1}{2}\arctan 2(\tau_0^{-1} + \tau_1^{-1})\omega/\tau_0^{-1}(\tau_0^{-1} + 2\tau_1^{-1}) - \omega^2] \qquad (4)$$

Table II
Protonated Phenyl Carbon Spin-Lattice Relaxation Times of BPA[a]

temp, °C	62.9 MHz			22.6 MHz		
	5 wt %	10 wt %	30 wt %	5 wt %	10 wt %	30 wt %
−20	152	143		77	73	
0	216	198		151	126	
20	322	278		262	217	
40	526	436	214	439	380	128
60	797	657	322	652	586	218
80	1088	933	498	933	931	378
100	1387	1320	721	1335	1172	620
120	2002	1943	1056	1720	1673	890

[a] All relaxation times in ms.

Table III
Methyl Proton Spin-Lattice Relaxation Times of BPA[a]

temp, °C	90 MHz			22.6 MHz		
	5 wt %	10 wt %	30 wt %	5 wt %	10 wt %	30 wt %
−20	42	44		22	20	
0	56	53		37	32	
20	92	74	80	63	51	
40	137	105	100	82	65	50
60	170	145	121	102	95	70
80	228	195	163	142	147	100
100	305	273	228	210	183	122
120	384	332	290	266	249	159

[a] All relaxation times in ms.

Table IV
Methyl Carbon Spin-Lattice Relaxation Times of BPA[a]

temp, °C	62.9 MHz			22.6 MHz		
	5 wt %	10 wt %	30 wt %	5 wt %	10 wt %	30 wt %
−20	47	42		25	23	
0	64	64		39	39	
20	104	92		89	74	
40	159	134	103	114	98	74
60	229	216	149	165	152	102
80	318	290	216	239	238	159
100	421	402	300	330	335	244
120	583	541	404	488	426	311

[a] All relaxation times in ms.

This new correlation function can be combined with phenyl group rotation and methyl group rotation to yield a composite correlation function if each of the three local motions is considered to be independent. This composite correlation function can be Fourier transformed to yield a spectral density function analogous to eq 2 except it contains the new form for segmental motion.

$$J(\omega) = AJ_a(\tau_0,\tau_1,\omega) + BJ_b(\tau_{b0},\tau_1,\omega) + CJ_c(\tau_{c0},\tau_1,\omega) \quad (5)$$

$$A = (3\cos^2\Delta - 1)^2/4$$

$$B = 3(\sin^2 2\Delta)/4$$

$$C = 3(\sin^4\Delta)/4$$

For stochastic diffusion

$$\tau_{b0}^{-1} = \tau_0^{-1} + \tau_{ir}^{-1}$$

$$\tau_{c0}^{-1} = \tau_0^{-1} + (\tau_{ir}/4)^{-1}$$

For a threefold jump

$$\tau_{b0}^{-1} = \tau_{c0}^{-1} = \tau_0^{-1} + \tau_{ir}^{-1}$$

The form of J_a, J_b, and J_c is the same as in eq 4 with τ_0 replaced by τ_0, τ_{b0}, and τ_{c0}, respectively.

From this point, the interpretation just parallels the one discussed for the three-bond jump. It starts with the adjustment of τ_0 and τ_1 to account for the phenyl proton relaxation data. Actually, because of the simpler functional form for segmental motion in the Weber–Helfand function, the data can realistically be fit as a function of temperature with a nonlinear least-squares program if an Arrhenius dependence is assumed for τ_0 and τ_1. After the segmental description is determined, the correlation time for phenyl group rotation is set from the phenyl carbon data, and the correlation time for methyl group rotation is set from the methyl carbon and proton data. Again the experimental relaxation times can be simulated to within about 10% or better; compilations of correlation times producing these simulations for BPA and chloral are given in Tables VIII and IX, respectively. An Arrhenius summary of correlation times produced by the simulation based on eq 5 is included in Tables VIII and IX.

Table V
Spin-Lattice Relaxation Times of a 10 wt % Solution of Chloral[a]

temp, °C	phenyl protons		protonated phenyl carbons	
	90 MHz	30 MHz	62.9 MHz	22.6 MHz
−20	718	255	144	69
0	597	239	173	104
20	625	275	225	151
40	591	318	330	226
60	709	427	461	371
80	837	521	629	526
100	1019	782	854	667
120	1176	831	1152	911

[a] All relaxation times are in ms.

Discussion

The descriptions of local motions in BPA and chloral just developed are reassuringly similar to the earlier studies. Segmental motion, phenyl group rotation, and methyl group rotation are all of similar time scales in BPA as they were before; and the time scales for BPA and chloral are also comparable to those reported earlier.[1,2] These general conclusions are not even dependent on which of the two models for segmental motion is employed.

Other general observations can be made. First, the new solvent $C_2D_2Cl_4$ is more viscous than the $CDCl_3$ used before; this would roughly account for the shift in all T_1's by a factor of 2–4 in going from $CDCl_3$ to $C_2D_2Cl_4$. Also the apparent activation energies increase by about 5 kJ, which is consistent with the nature of the solvent change. As was true in chloroform, at a concentration of 10 wt %, the correlation times for segmental motion, phenyl group rotation, and methyl group rotation are all quite similar in BPA. The possibility of cooperatively or gearing between the motions was raised after the initial observation.[1] However, it is also apparent in the new data that con-

Table VI
Simulation Parameters for BPA Using the Three-Bond Jump Model

temp, °C	m: 5 wt %	m: 10 wt %	m: 30 wt %	τ_h, ns: 5 wt %	τ_h, ns: 10 wt %	τ_h, ns: 30 wt%	τ_{irp}, ns: 5 wt %	τ_{irp}, ns: 10 wt %	τ_{irp}, ns: 30 wt %	τ_{irm}, ns: 5 wt %	τ_{irm}, ns: 10 wt %	τ_{irm}, ns: 30 wt %
−20	3	3		1.173	1.20		1.84	2.32		0.870	1.30	
0	3	3	5	0.624	0.685	2.10	0.810	1.00		0.500	0.480	
20	3	3	3	0.329	0.450	1.50	0.440	0.530		0.220	0.251	
40	5	5	3	0.195	0.321	0.700	0.228	0.230	0.855	0.120	0.146	0.144
60	7	5	3	0.111	0.185	0.483	0.152	0.170	0.413	0.0920	0.0745	0.0815
80	7	5	3	0.0788	0.119	0.337	0.104	0.108	0.215	0.0540	0.0430	0.0357
100	9	7	5	0.0470	0.0700	0.177	0.0800	0.0817	0.142	0.0350	0.0300	0.0231
120	9	7	5	0.0342	0.0530	0.123	0.0540	0.0550	0.0926	0.0241	0.0160	0.0112
E_a, kJ/mol				21	19	21	21	22	28	21	25	33
$\tau_\infty \times 10^{14}$, s				5.5	20	19	9.6	6.3	1.5	3.7	0.84	0.058
corr coeff				0.99	0.99	0.99	0.99	0.99	0.99	0.99	0.99	0.99

Table VII
Simulation Parameters for Chloral Using the Three-Bond Jump Model

temp, °C	m	τ_h, ns	τ_{irp}, ns
−20	5	1.70	1.96
0	3	0.833	1.18
20	3	0.490	0.791
40	3	0.336	0.475
60	3	0.235	0.290
80	5	0.137	0.200
100	5	0.0994	0.153
120	7	0.0707	0.108
E_a, kJ/mol		18	17
$\tau_\infty \times 10^{14}$, s		29	56
corr coeff		0.99	0.99

centration selectively affects the local motions. As concentration is raised from 5 to 30 wt %, the correlation time for segmental motion and phenyl group rotation increases, while the correlation time for methyl group rotation changes very little. This difference in concentration dependence is quite plausible since segmental motion and phenyl group rotation would sweep out a larger volume than methyl group rotation. At a concentration of 30 wt %, the segmental and phenyl correlation times are still quite similar but the correlation time for methyl group rotation is much shorter. It would appear that any cooperativity between methyl group rotation and the other motions is weak since concentration changes produce a ready separation. On the other hand, the continued similarity between the time scale of phenyl group rotation and segmental motion over a range of temperature and concentration leaves open the possibility of cooperativity between these two motions. Changing the concentration from 5 to 30 wt % shifts correlation times by a factor of 4 or less, and no quantitative interpretation of the effect will be undertaken until a larger concentration range is studied in other solvents.

As just mentioned, the similarity in correlation times between the BPA and chloral polycarbonates noted before[2] still holds. At 10 wt %, the correlation times for both phenyl group rotation and segmental motion are within a factor of 2 for both polymers. In chloral both motions are a little slower but the parallel between these two polymers is clear. The similarity in both polymers between the phenyl rotation and segmental motions suggests that the apparent phenyl group rotation might be produced by cis–trans isomerization by rotation about C–O bonds.[8] The rotations about a C–O bond cause the ring on the other side of the carbonate group to rotate about an axis inclined at an angle of less than 15° from the C_1C_4 axis. This motion essentially meets the geometric requirement imposed to define phenyl group rotation, i.e., that the proton dipole–dipole interaction between the 2–3 protons not be reoriented. If this pseudo phenyl group rotation is indeed what is being observed as phenyl group rotation, then it is not surprising that it parallels the time scale of segmental motion since it is produced by rearrangement of nearby backbone bonds.

The pseudo phenyl group rotation produced by rotation about the C–O bond would also explain the similarity in phenyl group rotation between chloral and BPA. MNDO calculations on the dichloroethylene unit[9] indicate a high barrier, 42 kJ to phenyl group rotation, but the pseudorotation about the carbonate unit is only a 10-kJ barrier. The MNDO calculations were made on small sections of chain so extrapolation to the polymer involves some uncertainty but the results are worthy of consideration.

Table VIII
Simulation Parameters for BPA Using the Weber-Helfand Model

temp, °C	τ_i, ns: 5 wt %	τ_i, ns: 10 wt %	τ_i, ns: 30 wt %	τ_v, ns: 5 wt %	τ_v, ns: 10 wt %	τ_v, ns: 30 wt %	τ_{irp}, ns: 5 wt %	τ_{irp}, ns: 10 wt %	τ_{irp}, ns: 30 wt %	τ_{irm}, ns: 5 wt %	τ_{irm}, ns: 10 wt %	τ_{irm}, ns: 30 wt %
−20	1.90	1.88		20.5	25.0		1.64	1.95		0.875	1.03	
0	1.10	1.32	3.10	12.0	18.8	44.0	0.730	0.850		0.430	0.440	
20	0.440	0.680	1.77	8.60	16.6	17.7	0.440	0.510		0.200	0.238	0.240
40	0.275	0.575	1.40	6.62	15.8	15.0	0.215	0.225	0.715	0.118	0.122	0.135
60	0.183	0.240	0.708	4.59	6.30	9.20	0.140	0.170	0.395	0.0802	0.0835	0.0850
80	0.121	0.175	0.415	3.15	3.10	5.65	0.0950	0.0960	0.220	0.0451	0.0453	0.0456
100	0.0897	0.112	0.285	1.97	2.47	3.22	0.0720	0.0750	0.135	0.0273	0.0274	0.0275
120	0.0685	0.0904	0.179	1.50	2.04	2.28	0.0450	0.0460	0.0890	0.0161	0.0164	0.0166
E_a, kJ/mol	20	19	21	15	16	21	21	22	27	23	24	26
$\tau_\infty \times 10^{14}$, s	13	28	30	1713	1603	384	8	6	2	2	1	1
corr coeff	0.99	0.99	0.99	0.99	0.94	0.99	0.99	0.99	0.99	0.99	0.99	0.99

Table IX
Simulation Parameters for Chloral Using the Weber–Helfand Model

temp, °C	τ_1, ns	τ_0, ns	τ_{irp}, ns
−20	1.80	30.0	2.12
0	1.63	11.1	1.07
20	0.933	6.75	0.685
40	0.630	4.70	0.406
60	0.373	2.97	0.259
80	0.255	2.11	0.180
100	0.176	1.53	0.140
120	0.134	1.19	0.0980
E_a, kJ/mol	17	18	18
$\tau_\infty \times 10^{14}$, s	94	409	40
corr coeff	0.99	0.99	0.99

The interpretations resulting from the two models for segmental motion can be compared. The primary parameter controlling the simulation in the three-bond jump model is the correlation time for segmental motion, τ_h. In this model the parameter m plays a secondary role. In the application of the Weber–Helfand model to the polycarbonate data, the primary parameter controlling the simulation is the correlation time for cooperative transitions, τ_1. The parameter τ_0 plays a minor role, which is easily noted in this case since it is much longer than τ_1. If we now compare the parameter in each simulation that is controlling the simulation, they are found to be comparable. This is quite apparent in the Arrhenius summaries in Tables VI–IX, where both activation energy and the prefactor are rather similar for τ_h and τ_1.

The similarity between τ_h and τ_1 can be rationalized to a certain extent. The three-bond jump model is based on a conformational transition that would be classified as highly cooperative since it is a crankshaft[10–12] though it is not a common transition according to the computer simulations that serve as the basis of the Weber–Helfand model. Cooperative transitions are lumped together in the Weber–Helfand correlation function under the time constant τ_1. Thus it would appear that the time constant for cooperative transitions in both models leads to nearly the same parameters in spite of the fact that the models are developed from quite different starting points. This lends more credence to the two models and also raises the question about the apparent dominance of cooperative transitions since both models rely primarily on them to account for the polycarbonate data. In the computer simulations of a polyethylene-type backbone that led to the Weber–Helfand model, cooperative transitions did not play such a dominant role in conformational relaxation. The difference in this interpretation of spin relaxation data in polycarbonates could be real and reflect the more complicated repeat unit; or it could merely be an artifact of as yet overly simplified models.

In the Weber–Helfand model the activation energies for single transitions and cooperative transitions are not too different as they ought to be if[3,9–11] the cooperative transitions are composed of two sequential single transitions as opposed to two simultaneous single transitions, i.e., a crankshaft. This fact favors the Weber–Helfand view over the three-bond jump model.

Another reassuring aspect of the interpretation is the relative constancy of the simulation parameters τ_{irp} and τ_{irm} when the description of segmental motion is changed. This implies that the separation of local motions based on repeat-unit geometry is at least consistent when the description of segmental motion is adequate.

Since both models for segmental motion lead to similar conclusions, which model should be routinely applied to interpret experimental data? The model by Weber and Helfand is superior to the three-bond jump model in ease of use. The Weber–Helfand model has a simple closed form with continuously variable parameters while the three-bond jump model has a variable that only takes on integer values so that both the correlation function and spectral density are written as a sum dependent on this integer variable. As mentioned, the quality of the simulations of experimental data is comparable although the Weber–Helfand model gave slightly more stable estimates of τ_{irm} as a function of concentration for BPA. On the other hand, the three-bond jump model did a slightly better job of simulating the T_1 minimum in the chloral phenyl proton data. Probably both models should be tested against a few more sets of data but at this time the Weber–Helfand model is preferable as having a sounder basis and easier applicability.

Acknowledgment. We are grateful to Dr. R. P. Lubianez for the synthesis of the partially deuterated BPA. We also thank Dr. E. Helfand for providing us with a preprint describing the new Weber–Helfand correlation function and for also providing the Fourier transform of the correlation function. The research was carried out with financial support of National Science Foundation Grant DMR-790677, of National Science Foundation Equipment Grant No. CHE 77-09059, and of National Science Foundation Grant No. DMR-8108679.

Registry No. (BPA-d_6)·(CH_2O_3) (copolymer), 86588-59-2; (BPA)·(CH_2O_3) (copolymer), 25037-45-0; (Chloral)·(CH_2O_3) (copolymer), 29057-43-0; (BPA-d_6)·(CH_2O_3) (SRU), 86588-81-0; (BPA)·(CH_2O_3) (SRU), 24936-68-3; (Chloral)·(CH_2O_3) (SRU), 31546-39-1.

References and Notes

(1) Jones, A. A.; Bisceglia, M. *Macromolecules* **1979**, *12*, 1136.
(2) O'Gara, J. F.; Dejardins, S. G.; Jones, A. A. *Macromolecules* **1981**, *14*, 64.
(3) Weber, T. A.; Helfand, E., submitted to *J. Chem. Phys.*
(4) Jones, A. A.; Stockmayer, W. H. *J. Polym. Sci., Polym. Phys. Ed.* **1977**, *15*, 847.
(5) Jones, A. A.; Robinson, G. L.; Gerr, F. E. *ACS Symp. Ser.* **1979**, *No. 103*, 271.
(6) Heatley, F. A. *Prog. NMR Spectrosc.* **1979**, *13*, 47.
(7) Lubianez, R. P.; Jones, A. A. *J. Magn. Reson.* **1980**, *38*, 331.
(8) Helfand, E., private communication.
(9) Jones, A. A.; O'Gara, J. F.; Inglefield, P. T.; Bendler, J. T.; Yee, A. F.; Ngai, K. L. *Macromolecules* **1983**, *16*, 658.
(10) Helfand, E. *J. Chem. Phys.* **1971**, *54*, 4651.
(11) Helfand, E.; Wasserman, Z. R.; Weber, T. A. *Macromolecules* **1980**, *13*, 526.
(12) Skolnick, J.; Helfand, E. *J. Chem. Phys.* **1980**, *72*, 5489.